Electrogastrogram-based detection of cybersickness with the application of wavelet transformation and machine learning: a case study

Ilija V. Tanasković[a], *Nenad* B. Popović[b], *Jaka* J. Sodnik[c], *Sašo* J. Tomažič[d], *Nadica* S. Miljković[e]

[a]University of Belgrade, School of Electrical Engineering, Belgrade, Republic of Serbia +
The Institute for Artificial Intelligence Research and Development of Serbia, Novi Sad, Republic of Serbia,
e-mail: ilija.tanaskovic@ivi.ac.rs, **corresponding author**,
ORCID iD: https://orcid.org/0000-0002-6488-4074

[b] University of Belgrade, School of Electrical Engineering, Belgrade, Republic of Serbia,
e-mail: nenad.pop92@gmail.com,
ORCID iD: https://orcid.org/0000-0002-5221-1446

[c] University of Ljubljana, Faculty of Electrical Engineering, Ljubljana, Republic of Slovenia,
e-mail: jaka.sodnik@fe.uni-lj.si,
ORCID iD: https://orcid.org/0000-0002-8915-9493

[d] University of Ljubljana, Faculty of Electrical Engineering, Ljubljana, Republic of Slovenia,
e-mail: saso.tomazic@fe.uni-lj.si,
ORCID iD: https://orcid.org/0000-0002-2968-8879

[e] University of Belgrade, School of Electrical Engineering, Belgrade, Republic of Serbia +
University of Ljubljana, Faculty of Electrical Engineering, Ljubljana, Republic of Slovenia,
e-mail: nadica.miljkovic@etf.bg.ac.rs,
ORCID iD: https://orcid.org/0000-0002-3933-6076

https://doi.org/10.5937/vojtehg73-51577

FIELD: electronics, information technology
ARTICLE TYPE: original scientific paper

Abstract:

Introduction/purpose: The application of virtual reality (VR) and simulation technologies in military training offers cost-effective and versa-

ACKNOWLEDGMENT: This research was partially funded by the Slovenian Research Agency within the research program ICT4QoL–Information and Communications Technologies for Quality of Life, grant number P2-0246. Nadica Miljković was partly supported by the Ministry of Science, Technological Development and Innovation of the Republic of Serbia [Grant No. 451-03-65/2024-03/200103].

tile approach to training enhancement. However, prevalence of cybersickness (CS), characterized by symptoms such as nausea, limits their widespread use.

Methods: This study introduces objective parameters for the detection of CS using three-channel electrogastrogram (EGG) recording from one specific subject and assesses the independence and linear correlation for appropriate channel selection. The paper employs a 3-level discrete wavelet transformation (DWT) on the chosen channel to identify key parameters indicative of gastric disturbances. Furthermore, the paper investigates recovery from CS following VR and examines the application of unsupervised machine learning (ML) for segmenting EGG into baseline and CS, utilizing significant features previously identified.

Results and discussion: The analysis reveals no significant differences across EGG channels and moderate to low linear correlation between channel pairs. The feature selection demonstrates that the root mean square of the amplitude as well as the maximum and mean values of the power spectral density (PSD) calculated on all DWT coefficients, are effective for CS detection while the dominant EGG scale could not indicate CS for any level of decomposition. Furthermore, recovery signs appear approximately 8 minutes after the first VR experience supporting the idea of conducting multiple sessions the same day i.e., intensive VR-based training.

Conclusions: The unsupervised ML shows potential in identifying CS-affected EGG signal segments with feature extraction based on DWT, offering a novel approach for enhancing the prevention of CS occurrence in VR-based military training and other VR-related environments.

Keywords: cybersickness, discrete wavelet transform, electrogastrography (EGG), feature selection, machine learning, military training, power spectral density, virtual reality.

Introduction

The application of simulation technologies in the training of military personnel has been around since the 1950s. In recent years due to the rapid development of graphics, the application of virtual reality (VR) has emerged as a promising approach in the army (Bruzzone & Massei, 2017; Tecknotrove. 2023). The application of simulators in the military offers a cost-effective, rapid, and versatile method for preparing personnel for a wide range of scenarios including psychomotor training (*e.g.*, shortening reaction time), cognitive learning (*e.g.*, solving tactical problems), and affective learning (*e.g.*, adapting the training process to the students' abilities

and interests) (Bruzzone & Massei, 2017; Vlačić et al., 2020). However, the widespread applicability of these advanced training tools is limited to the prevalence of cybersickness (CS). The mismatch between visual and vestibular sensors is commonly assumed to cause CS, while CS is characterized by symptoms similar to motion sickness (MS), including nausea, disorientation, and headache. Therefore, CS emerges as a significant barrier to an immersive experience provided by simulation and VR technologies (Dennison et al., 2016; LaViola, 2000; Miljković et al., 2019; Gruden et al., 2021). Moreover, CS symptoms can manifest during or after exposure to virtual environments, posing a particular concern for VR-based training adoption. The recognition and mitigation of CS are of paramount importance, especially in contexts where the physical and cognitive readiness of military personnel is non-negotiable (NATO Science and Technology Office. 2021).

Traditional methods for investigating CS have predominantly relied on subjective reporting of symptoms through questionnaires (Tian et al., 2023; Dennison et al., 2016; Gruden et al., 2021). Such a qualitative approach, while providing insights, is fraught with limitations, including the potential for subjectivity and bias (Dennison et al., 2016). Given that many CS symptoms, such as nausea, are associated with the smooth muscles of the stomach, the electrogastrogram (EGG) emerges as a promising objective measure (Dennison et al., 2016; Tian et al., 2023; Miljković et al., 2019; Popović, 2021). EGG, capable of capturing changes in gastric myoelectrical activity, offers a direct link to the physiological underpinnings of CS, bypassing the subjectivity of self-reported measures and as a supplementary objective measure to commonly used questionnaires. (Miljković & Sodnik, 2023).

The exploration of EGG as a diagnostic tool for CS started a few decades ago, with a growing potential. Traditional EGG analysis is focused on changes in the EGG amplitude in both time and frequency domains. Additionally, frequency shifts in power spectral density (PSD) towards specific frequency bands indicative of gastric distress, such as bradygastria (slow gastric waves) and tachygastria (rapid gastric waves) could be used as CS indicators (Popović, 2021; Dennison et al., 2016). These features have laid the groundwork for understanding the physiological responses associated with CS, yet the complexity of EGG signals calls for more sophisticated analytical techniques to capture their assessment potential fully.

Recent advances have introduced machine learning (ML) models as a complement to the traditional statistical approaches for assessing the changes in the EGG dynamics. Despite this, literature shows that investigations focusing exclusively on the EGG features for CS detection through ML are sparse (Yang et al., 2022). A few studies have experimented with integrating ML models with the EGG features, but only in combination with the features derived from multiple physiological and behavioral measurements (*e.g.*, EEG, electrocardiogram – ECG, posture, electrodermal activity – EDA, etc.) to estimate the levels of CS during the simulation or the Simulator Sickness Questionnaire (SSQ) scores (Dennison et al., 2016, 2019; Keshavarz et al., 2022). However, these studies (Dennison et al., 2016, 2019; Keshavarz et al., 2022) found that using the EGG features alone did not yield significant results, highlighting a notable gap in the research and showing a promising opportunity for future investigations with demonstrated the potential of the EGG features. Jakus et al. (2022) successfully employed ML models to detect the occurrence of nausea, one of the primary symptoms of CS. This emerging evidence indicates that, although the application of ML to EGG data for CS detection is still in its early stages, it could be a promising approach to pair ML with innovative feature engineering for extracting information of interest. The significant challenge in applying ML to detect the onset of CS is due to the lack of reliable real-time labels required for supervised learning. Labeling is predominantly conducted using questionnaires, which poses limitations for real-time analysis. The SSQ, widely used as a gold standard for assessing CS, is administered only before and after a VR experience (Miljković & Sodnik, 2023; Merchant & Kirollos, 2022; Tian & Boulic, 2024). While effective in determining whether CS occurred, the SSQ lacks the temporal resolution required for training supervised models. To address this, the Fast Motion Sickness Scale (FMS) has been introduced, as a good substitution due to the high correlation to the SSQ (Keshavarz & Hecht, 2011), involving participants self-reporting their CS levels at regular intervals, typically every minute (Tian & Boulic, 2024; Merchant & Kirollos, 2022; Dennison et al., 2016, 2019). Despite its higher temporal resolution, the FMS is subjective and susceptible to bias, as participants may underreport symptoms to appear resilient or may delay acknowledging discomfort (Tian & Boulic, 2024; Merchant & Kirollos, 2022). Considering these challenges, unsupervised ML emerges as a promising approach for CS detection using the EGG sig-

nals. By not relying on potentially unreliable or biased labels, unsupervised methods can detect intrinsic patterns and variations in the data, providing a more objective and accurate analysis of CS-related changes in gastric activity (Miljković & Sodnik, 2023; Tian & Boulic, 2024). Moreover, an objective method for assessing CS is crucial for enhancing the widespread adoption of VR technologies, particularly in military training, where it enables personnel to gain experience in controlled environments that closely simulate realistic scenarios (Kuhl et al., 1995; Miljković & Sodnik, 2023).

This paper proposes the use of discrete wavelet transformation (DWT), a method well-suited for analyzing non-stationary signals with the ability to analyze changes in both time and frequency without the necessity of compromise imposed by the short-time Fourier transform (STFT) including a fixed window size leading to a trade-off between time and frequency resolution, poorer localization for non-stationary signals, and less effective handling of rapid signal changes. Wavelet-based features have already shown promise in identifying disturbances in gastric activity in diabetic patients by allowing for the decomposition of the EGG signal into components that can be analyzed with great precision (Tokmakçi, 2007; Kara et al., 2005). To our knowledge, this is the first paper dealing with CS detection using wavelet transformation. Through this approach, we seek to contribute to the fields of defense sciences and VR technologies, offering insights that could enhance the efficacy and safety of VR-based military training programs, as well as other VR applications.

Aim of the study

This paper is an extension of the previous research (Popović, 2021; Miljković et al., 2019; Miljković & Sodnik, 2023) which investigated the application of the EGG signals for CS detection. The focus of the paper is on the EGG analysis from a single subject who experienced severe symptoms of nausea which led to the cessation of VR experience. The novelty of the proposed method lies in the adoption of wavelet-based features, which have already been utilized in the detection of disturbances in EGG signals in subjects with diabetes (Tokmakçi, 2007; Kara et al., 2005). Also, our methodology explores the indication of recovery from CS with EGG (hereinafter stomach recovery) after VR experience and the possible application of unsupervised ML models to segment signals into two groups (baseline and CS). In this study, the following research questions are presented:

1. Can we use wavelet-based features to detect the CS segments of the EGG recording?
2. Concerning the fact that the three-channel EGG is available for recording, can we use automatic detection of the most suitable channel?
3. Given the features observed in EGG, can a subject achieve recovery following VR exposures in a relatively short break (10 minutes) as proposed by Popović (2021) after experiencing CS?
4. Can an unsupervised ML model be used for the recognition of EGG recording to the baseline and CS segments in the time domain?

Methods and materials

The summary of the proposed methodology is shown using a block diagram in Figure 1. The proposed pipeline begins with a statistical comparison of the EGG channels to assess independence and linear correlation. This is followed by the extraction of features which are subsequently analyzed to identify reliable indicators of CS segments and recovery segments by applying appropriate methods for feature extraction and selection. In the final step, unsupervised segmentation is utilized to divide the signal into two distinct clusters (CS and recovery), facilitating a clearer understanding of the data. The feature extraction step is implemented using MATLAB 2023b (The Mathworks Inc., Natick, USA), while the remaining steps (including channel comparison, feature selection, CS recovery, and unsupervised ML segmentation) are implemented in Python 3.9 (Van Rossum & Drake, 1995) using libraries numpy (Harris et al., 2020) and pandas (McKinney, 2010) for data manipulation; matplotlib for visualization (Hunter, 2007); scipy for signal filtering and statistic tests (Virtanen et al., 2020); statsmodels (Seabold & Perktold, 2010) for the correction of p-value for multiple comparisons, and scikit-learn for unsupervised ML (Pedregosa et al., 2011).

Dataset and preprocessing

This case study is focused on one female subject who experienced severe CS symptoms during VR exposure. The subject signed the Informed Consent in accordance with the Declaration of Helsinki. The study is performed in compliance with the Code of Ethics for researchers and the Guidelines for ethical conduct in research involving people issued by

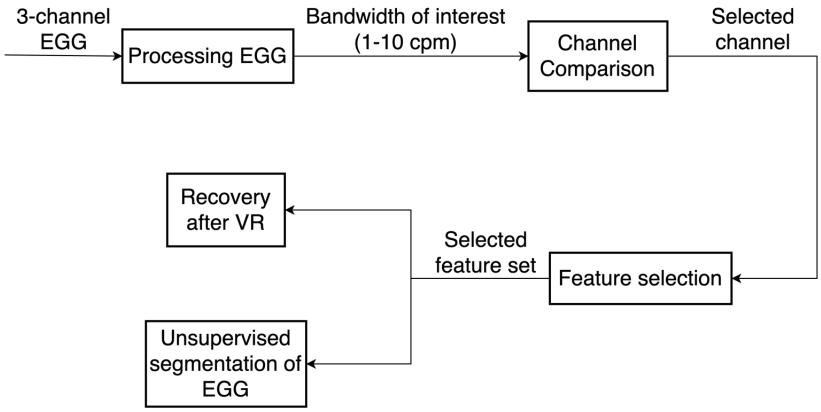

Figure 1 – Block diagram of the proposed methodology. cpm – cycle per minute

the University of Ljubljana. A detailed description of hardware and software setup that is used in VR-related study is provided by (Miljković et al., 2019). The sampling frequency of the recorded signal is set to 2 Hz and the gain is set to 1000. The recording process was segmented based on the participant's engagement with the VR equipment, encompassing a pre-VR baseline segment of 8 minutes (B1), the first VR exposure of 4 minutes (VR1), a 10-minute pause (B2), a second VR session (VR2) planned for 6 minutes and 20 seconds but terminated after 2 minutes due to the emergence of severe CS symptoms, and a final 8-minute post-VR baseline (B3). VR1 contains Rock Falls VR with an included roller coaster session lasting 4 min while VR2 contains a T-Rex Kingdom VR roller coaster session lasting 6 min and 20 s. (Miljković et al., 2019; Popović, 2021; Meta. 2024)

These segments are delineated solely based on the timing of VR equipment usage, which does not exclude the possibility of CS effects manifesting outside VR periods. The signal is filtered using one 5^{th} order bandpass Butterworth filter to roughly extract the bandwidth of interest for the EGG signal between 1 and 10 cpm (cycles per minute) respectively (Dennison et al., 2016; Miljković et al., 2019). The filtering is conducted in both forward and backward directions to achieve zero-phase filtering.

Channel comparison

The EGG is captured using three channels, as outlined in (Miljković et al., 2019; Popović, 2021; Gruden et al., 2021). The electrode for channel

(ch) 1 is located above the stomach's lesser curvature, an area characterized by a lower density of Cajal interstitial cells compared to the pacemaker region adjacent to the greater curvature, where the electrode for ch3 is positioned. A common electrode is affixed along the line connecting the navel to the sternum, 8 cm above the navel. Ch2 electrode is strategically placed equidistant from ch1 and ch3, ensuring the angles between them are identical. To prevent potential breathing-induced artifacts, all three electrodes are positioned 8-9 cm from the common electrode, carefully avoiding placement over the ribs. The reference electrode is secured to the electrically inactive tissue atop the iliac bone. (Popović, 2021)

Initially, a Friedman chi-square test is conducted to assess the comparability of samples across the three channels. In case the Friedman test rejects the null hypothesis, a post-hoc analysis is performed utilizing the Wilcoxon signed-rank test for pairwise signal comparisons. The calculated *p*-values are adjusted for multiple comparisons using Bonferroni's correction method to mitigate the risk of Type I errors setting the threshold of adjusted *p*-value on 0.05. Furthermore, to investigate the information that each channel may provide, the correlation between channel pairs is explored using Pearson's coefficient and scatterplots, aiming to deepen our understanding of the inter-channel relationships in the presence of CS.

Feature selection

Our methodology adopts amplitude- and frequency-based features proposed by the literature (Gruden et al., 2021; Miljković et al., 2019; Tian et al., 2023; Dennison et al., 2016), but instead of extracting frequency bands using classical filtering or STFT, the use of DWT is proposed. The detailed description of the features is provided in the subsection on Feature extraction. This substitution is particularly advantageous for its ability to provide variable resolution across multiple scales, a feature not available with the STFT which uses a fixed window size or with classical frequency band filtering that lacks temporal resolution. This adaptive resolution of DWT allows for smaller windows at higher frequencies to capture rapid changes, and larger windows at lower frequencies to better resolve slower waves. These capabilities make DWT highly suitable for the complex, non-stationary characteristics of EGG signals in CS detection, offering a more nuanced analysis by adapting to the varying dynamics of the signal. (Tokmakçi, 2007; Kara et al., 2005)

Discrete wavelet transformation

DWT is a mathematical tool utilized for the decomposition of signals into a hierarchical structure of frequency bands, enabling detailed analysis with localization in both time and frequency domains. It operates by iteratively applying low-pass and high-pass filters to the samples, thereby extracting its detail coefficients (from the highpass filter) and approximation coefficients (from the lowpass filter) at each level of decomposition. The decomposition process is visualized in Figure 2 where 2↓ stands for downsampling with factor 2 and *cd1* stands for the detail coefficient of the first level decomposition.

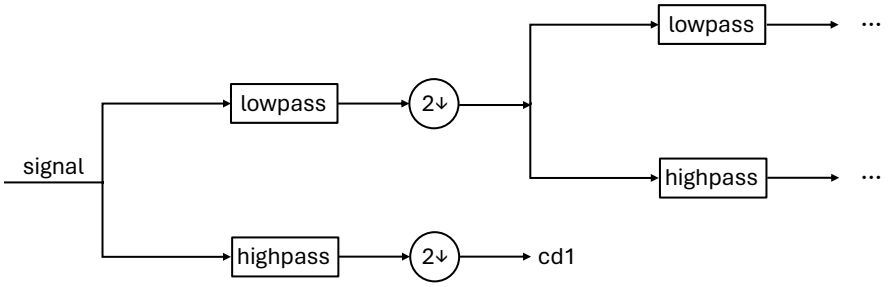

Figure 2 – Block diagram of discrete wavelet transform

The reason for downsampling the signal is to fulfill the sampling theorem—which mandates that the sampling frequency should be at least twice the highest frequency in the signal to prevent aliasing and since half of the samples are removed, the effective sampling rate is reduced in half. The process continues as many times as the levels of decomposition are needed. The remaining coefficients, after the j number of decomposition, are called approximation coefficients and their length as well as the length of the last detail coefficients are $2j$ times the length of the original signal. The adaptability of the DWT coefficients, facilitated by the choice of wavelet basis functions, allows for the optimization of signal representation, making it particularly effective for analyzing signals with transient or non-stationary characteristics. (Akansu & Haddad, 2001; Percival & Walden, 2006; Valens, 1999)

Feature extraction

Our study is focused on one subject and in order to conduct appropriate feature selection we augment our dataset by employing feature extraction on multiple consecutive windows with a length of 60 s and 50% overlap creating one data interval per window to capture the nuances and characteristics on more stationary parts of the signal. This resulted in 59 data intervals for the entire signal. The EGG signal is decomposed using the 'db3' Daubechies wavelet with three levels of decomposition which results in three detailed coefficients (cd) and one approximation coefficient (ca) (Tokmakçi, 2007). Based on the literature review, four types of features have been identified as appropriate for the analysis:

- root means square (RMS) of the amplitude (Gruden et al., 2021; Popović et al., 2019b),
- maximum of PSD (Gruden et al., 2021; Jakus et al., 2022),
- mean of PSD (Tokmakçi, 2007), and
- dominant scale.

The RMS is a standard metric for quantification of amplitude variations in biomedical signals (Cacioppo et al., 2007). Studies (Popović, 2021; Gruden et al., 2021; Jakus et al., 2022) have demonstrated that the onset of CS is associated with increased gastric activity, characterized by an elevated amplitude. The RMS is employed to quantify this amplitude increase, facilitating the detection of CS onset. Additionally, it is used to monitor the recovery of the amplitude to the baseline level, serving as an indicator of the recovery. The maximum of PSD also referred to as the dominant power, identifies the highest power concentrated at a specific rhythm (Popović, 2021; Gruden et al., 2021). An increase in the signal amplitude and the RMS during CS periods is expected to correspond with an increase in the maximum of PSD, making it a good indicator in distinguishing between normal and disturbed gastric rhythms. Similarly, the changes in PSD can be effectively captured by calculating the mean of PSD. CS is associated with rapid and unstable gastric rhythms (tachygastria) where the stomach becomes atonic and lacks frequency stability (Kara et al., 2005). Consequently, the PSD spectrum may become more dispersed, lacking a single dominant peak (Gruden et al., 2021; Dennison et al., 2016; Popović et al., 2019b). Therefore, an increase in overall spectral power should be expected, not just an increase in the dominant power. This highlights the

complementary nature of the mean PSD to the maximum PSD. As features of PSD, both the maximum and the mean PSD are anticipated to reflect elevated power with the onset of CS and a return to nominal levels as indicators of recovery, while the mean is more sensitive to changes in PSD. In addition to magnitude-based measures, the dominant scale is proposed as a feature in the assessment of EGG recordings. The dominant scale, defined as the scale at which the power PSD of the wavelet coefficients reaches its maximum, is proposed as the DWT counterpart to the dominant frequency obtained using the STFT analysis. This feature aims to locate the primary oscillation of smooth muscle cells by identifying the argument of the maximum PSD at each level of decomposition, effectively pinpointing the dominant rhythm on the subband. Since the dominant frequency has established itself as a standard feature for detecting the onset of CS, with stomach activity shifting from normal gastric rhythms to tachygastric bands (Popović, 2021; Gruden et al., 2021; Kim et al., 2005; Tian et al., 2023), the dominant scale is hypothesized to show similar potential. It is expected to increase with the onset of CS and return to normal levels upon recovery.

These features are extracted from the preprocessed signal and all four coefficients (three cds and one ca) resulting in a total of 20 features. By incorporating DWT in the feature extraction process, the emphasis is placed on its inherent filter bank properties. This approach allows for the decomposition of the original EGG signal into multiple frequency bands and enables the tracking of changes indicative of CS. The PSD-based features are calculated using MATLAB *pwelch* function with a 10-sample long Kaiser window with a 50% overlap and parameter beta of 2.5 which indicate stronger attenuation of the side lobes. The flexible Kaiser window function is selected as it can be adjusted to provide different transition widths (*i.e.*, sharpness) by choosing the appropriate parameter (beta) to set the trade-off between the main lobe width and the peak side lobe level (Kaiser & Schafer, 1980; Oppenheim, 2008; Lee & Kuo, 2001). Since a majority of other EGG-related studies used the von Hann window function (Kara et al., 2005; Tian et al., 2023; Tokmakçi, 2007), we compared the results for the application of both the Kaiser and von Hann window. The MATLAB function *pwelch* is used to estimate the PSD in the proposed implementation. The scaling factor inherent in DWT is accounted for by adjusting the signal sampling rate at each level of decomposition. Starting from the original signal rate, the

sampling rate is halved at each successive level: beginning at 2 Hz, then 1 Hz for the first level of decomposition, 0.5 Hz for the second level, and 0.25 Hz for the third level. This downsampling is a critical step in utilizing DWT, as described by Percival & Walden (2006) and Valens (1999). The dominant scale is determined as the argument of the maximum value of PSD, reflecting the peak position within the spectral content. Adjusting the sampling rate at each level ensures that the concept of scale is linked to the frequency bands of the decomposed signal, effectively bridging these two key aspects of wavelet analysis (Percival & Walden, 2006; Valens, 1999).

Identifying features appropriate for the detection of CS segments

In this phase of our research, the features from the EGG recordings that could be indicative of CS are identified. The structure of our case study data collection alternated between the baseline and VR segments, comprising three baselines and two VR segments in total. Given the uncertainty regarding the subject's recovery from the initial VR exposure (which will be investigated later), our analysis for CS detection is deliberately confined to B1 and VR1 segments. According to the timeline detailed in a protocol proposed by Popović (2021), the initial baseline segment spanned 8 minutes, followed by a 4-minute VR session. The feature extraction methodology involved using overlapping windows to generate a single data interval, which is then categorized into the corresponding segment (baseline or VR) based on the majority of the windows duration.

To discern features that significantly differentiate between the B1 and VR1 segments, the non-parametric Mann-Whitney U test is employed. Given the nature of the problem, which involves comparing data intervals before and after an event (the start of VR1), a statistical test designed for repeated measurements would be more suitable. However, because the number of data intervals in the two groups is not equal, the Mann-Whitney test was initially used. To confirm these findings, the analysis also utilizes the Wilcoxon signed-rank test, which is appropriate for repeated measures (McKnight & Najab, 2010; Woolson, 2005), and equalizes the number of samples by excluding the first few data intervals from B1 to match the number of intervals in VR1. This approach allowed us to validate the robustness of our feature selection while addressing the constraints of unequal sample sizes. The Bonferroni correction is applied to adjust the p-values to avoid Type I error and set a threshold for adjusted (adjusted) p-values at

0.05. This statistical rigor ensures the reliability of our findings, highlighting features with a genuine association with CS, thereby advancing our understanding of its detection through EGG signals. Further steps of the proposed pipeline are conducted using only statistically significant features determined in this step.

EGG recovery after the VR experience

A notable methodological variation introduced by Popović (2021) in the study design was the scheduling of both VR sessions on the same day, diverging from the approaches of Miljković et al. (2019) and Tian et al. (2023), which spaced the multiple with at least one day apart. Despite incorporating a 10-minute pause between the VR sessions, this adjustment prompts an inquiry into whether the stomach smooth muscles fully recovered and whether the data interval distribution during B2 mirrors that of B1. The comparative analysis is conducted by assessing each data interval from B2. This involved assessing whether each feature fell within the 5^{th} and 95^{th} quantiles of the distribution observed in B1. For a data interval to be considered as part of a distribution B1, it is determined that at least two-thirds of its features must reside within the specified quantile range. Such an analysis is pivotal for validating the consistency of the subject's response across sessions and for reinforcing the reliability of the data collected after VR1.

Unsupervised segmentation of the EGG signal

This step in our methodology employs unsupervised ML for the segmentation of data intervals into two clusters: baseline and VR. Due to the study retrospective nature and the absence of real-time CS labels, unsupervised learning was selected as an appropriate approach. This application aims to complement the statistical analysis provided in the previous step where the degree of recovery of each data interval is tested. Employing ML aims to explore whether data intervals across the three baseline segments naturally group together and whether the data intervals from both VR sessions exhibit similar patterns, potentially clustering them into a single, unified group.

For this task, the KMeans model is selected, known for simplicity and efficiency while assigning data in two clusters. The model decides based

on the predefined number of centroids (in our case two: baseline and VR) and iteratively assigning each interval to a specific centroid to minimize the inertia, which is defined as the mean squared distance between each sample and its closest centroid. One of the drawbacks of the KMeans is the sensitivity in the initialization of centroids, which is overcome using multiple initializations (setting *n_init* to a default value of 10) (Géron, 2022; Pedregosa et al., 2011). This ensures that the algorithm is independently initialized 10 times, with each run starting from a different set of initial centroids. The final model is automatically selected based on the inertia, with the KMeans class retaining the model with the lowest inertia after all 10 runs. (Géron, 2022; Pedregosa et al., 2011)

Results

The Friedman's chi-square test reveals a significant difference between the samples originating from three channels, yielding a chi-square value of 9.30 and a *p*-value of approximately 0.01. The subsequent post-hoc analysis, detailed in Table 1 and conducted using the Wilcoxon signed-rank test indicates no significant differences between the samples across multiple channels.

Table 1 – Results of the post-hoc test (Wilcoxon signed rank test) are conducted after the Friedman test. The table shows the p-value, the adjusted p-value, and whether the null hypothesis is rejected

Pairs of channels (ch)	*p*-value	adjusted *p*-value	Rejected null hypothesis
ch1 vs. ch2	0.076	0.229	False
ch2 vs. ch3	0.767	1.000	False
ch1 vs. ch3	0.888	1.000	False

The relationship between the channels is further investigated using the Pearson correlation coefficient and scatter plots of pairs of signals. The Pearson correlation coefficients between channels are 0.63, 0.33, and 0.13 for ch1 vs. ch2, ch2 vs. ch3, and ch1 vs. ch3, respectively. The scatterplots of pairs of signals are presented in Figure 3.

A crucial aspect of our methodology involves identifying features that effectively distinguish between B1 and VR1 segments. The feature selection process is conducted in two scenarios. The first scenario used only the features from ch1 due to its position, which is least prone to noise, as suggested by Miljković et al. (2019) and Popović et al. (2019b). In the sec-

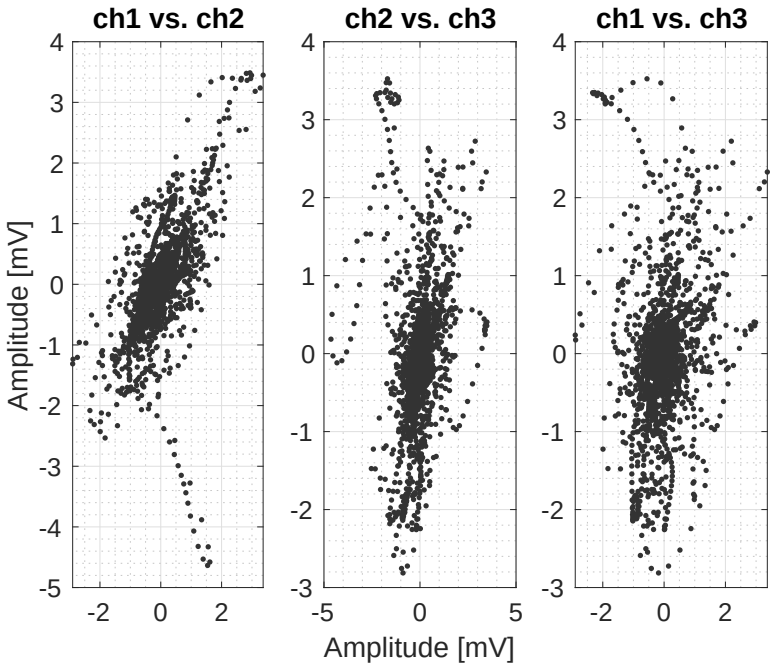

Figure 3 – Scatter plot of the pairs of the signal channels

ond scenario, combined features from ch1 and ch3 are used because ch3 has a low correlation with ch1 (0.13), indicating potential and additional valuable information, even though the analysis using the Wilcoxon signed-rank test showed no significant differences between the samples across multiple channels. To achieve this, the Mann-Whitney test is employed for feature selection, with the outcomes of this evaluation presented in Table 2. Additionally, the statistical analysis is performed on the features from both ch1 and ch3 and the results are presented in Table 3. The features demonstrating statistical significance, indicated by an adjusted *p*-value of less than 0.05, are highlighted in bold. Moreover, the results of feature selection using the Wilcoxon signed-rank test, conducted on the features from ch1 alone, as well as the combination of ch1 and ch3, confirm the findings of the Mann-Whitney test, with all features, except the features based on the dominant scale, showing statistically significant differences between B1 and VR1. Consequently, based on the results from Table 2 and Table 3, which indicate no significant difference in the selected features distinguishing between B1 and VR1 using either only features from ch1 or the

combined use of ch1 and ch3, a further analysis was carried out using only the features from ch1, as proposed by Miljković et al. (2019) and Popović et al. (2019b).

Table 2 – Results of feature selection using statistical tests conducted on channel 1. The Table shows the feature name, the p-value, and the adjusted p-value. The statistically significant features that could be used to discriminate between baseline and VR are marked in bold.

Feature	Decomposition level	*p*-value	Adjusted *p*-value
RMS amplitude value	processed signal	<0.001	**0.007**
	cd1	<0.001	**0.002**
	cd2	<0.001	**0.002**
	cd3	<0.001	**0.004**
	ca3	<0.001	**0.010**
Max value of PSD	processed signal	<0.001	**0.007**
	cd1	<0.001	**0.001**
	cd2	<0.001	**<0.001**
	cd3	<0.001	**<0.001**
	ca3	<0.001	**0.002**
Mean value of PSD	processed signal	<0.001	**0.007**
	cd1	<0.001	**0.001**
	cd2	<0.001	**<0.001**
	cd3	<0.001	**<0.001**
	ca3	<0.001	**0.002**
Dominant Scale of PSD	processed signal	1.000	1.000
	cd1	0.138	1.000
	cd2	0.098	1.000
	cd3	0.176	1.000
	ca3	0.532	1.000

Through the analysis comparing each of the 19 data intervals from B2 against the distribution derived from B1, it is determined that only 5 data intervals from B2 could be considered recovered. The recovery process after VR1 is visually represented in Figure 4, where the data intervals with recovered muscle cells are indicated with the orange color. Specifically, the 6^{th}, 7^{th}, 17^{th}, 18^{th}, and 19^{th} intervals from B2 show similarity with the distribution of B1. Based on Figure 4, the 6^{th} and 7^{th} data intervals correspond to time between 2 minutes and 30 s and 3 minutes and 30 s after VR1 stopped. However, since the 6^{th} and 7^{th} intervals are followed by intervals that do not meet the recovery criteria (i.e. show similarity with the distribution of B1) then the 6^{th} and 7^{th} intervals are considered transient or outliers and are thus not indicative of a stable state. The 17^{th} interval could be considered the first which resembles the distribution of B1 and from the

Table 3 – The results of feature selection using statistical tests conducted on features integrated from channels 1 and 3. The Table shows the feature name, p-value, and adjusted p-value. The statistically significant features that could be used to discriminate between baseline and VR are marked in bold.

Feature	Decomposition level	*p*-value	Adjusted *p*-value
RMS amplitude value	processed signal	<0.001	**<0.001**
	cd1	<0.001	**<0.001**
	cd2	<0.001	**<0.001**
	cd3	<0.001	**<0.001**
	ca3	<0.001	**<0.001**
Max value of PSD	processed signal	<0.001	**<0.001**
	cd1	<0.001	**<0.001**
	cd2	<0.001	**<0.001**
	cd3	<0.001	**<0.001**
	ca3	<0.001	**<0.001**
Mean value of PSD	processed signal	<0.001	**<0.001**
	cd1	<0.001	**<0.001**
	cd2	<0.001	**<0.001**
	cd3	<0.001	**<0.001**
	ca3	<0.001	**<0.001**
Dominant Scale of PSD	processed signal	1.000	1.000
	cd1	0.072	1.000
	cd2	0.035	0.713
	cd3	0.095	1.000
	ca3	0.472	1.000

17th to the 19th data intervals it can be assumed that the muscle cells of the stomach are recovered. Based on this finding, as well on Figure 4, it is assumed that the recovery is completed 8 minutes after VR1 stopped.

The last step in our pipeline is unsupervised segmentation of the EGG signal. The overlapped windows for the extraction of features resulted in 59 data intervals. The models divide 47 intervals in the first cluster and 12 intervals in the second cluster. The visual representation of the clustering results is shown in Figure 5 using different colors. The majority cluster, containing 47 data intervals, is not marked with color, while the intervals that belong to the minority cluster are colored in orange. Since overlapping windows are used, in cases where two consecutive and overlapped windows are clustered in two different groups, it is considered to be the transition between the states and that part of the signal is colored in wheat (light orange). According to the clusterization results, 25% of VR1 are categorized under the VR segment, while 50% of data intervals originating from VR2 are grouped as VR segments. Based on Figure 5, during VR1 the initial

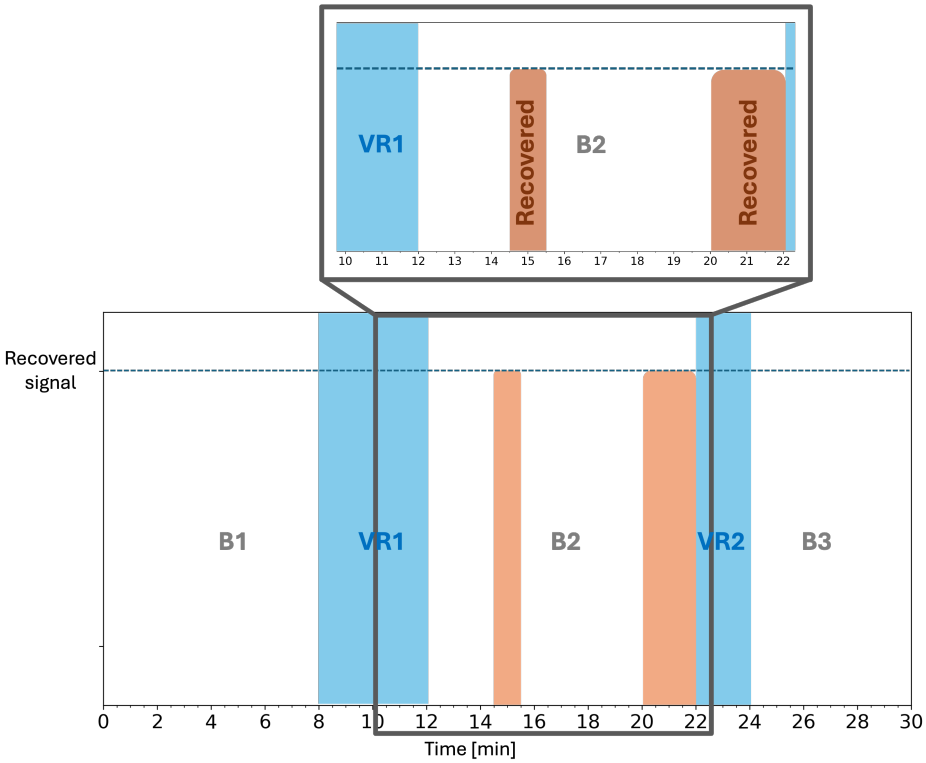

Figure 4 – Visual representation of the recovery process after the first VR experience. The light brown color indicates the recovered data intervals, while the blue color indicates the VR experience.

cluster identified as CS is likely due to movement artifacts from mounting the VR headset or to the emotional response to VR (Cacioppo et al., 2007), which were captured by the EGG signals and misclassified by the model. Notably, the latter part of VR1 did not form a distinct CS cluster, possibly because the CS symptoms were milder compared to the severe symptoms experienced during VR2 that led to the session termination. These observations highlight the models sensitivity to both physiological artifacts, emotional response and varying intensities of CS symptoms. These clusters were identified through unsupervised learning applied to the EGG signals, with no real-time feedback from the participants. The model segmented the data solely based on the distribution within the feature set, uncovering intrinsic patterns potentially associated with CS.

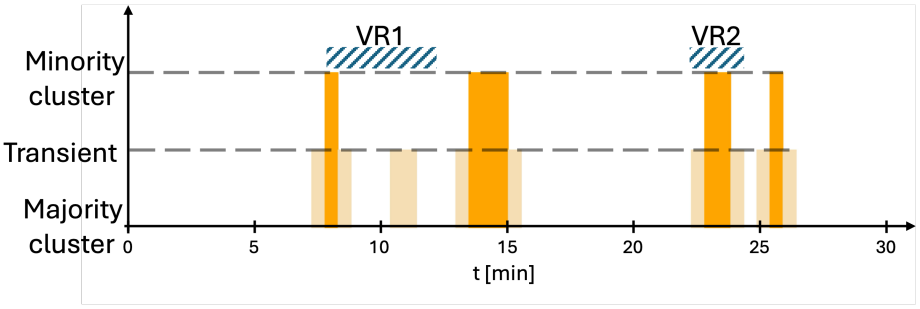

Figure 5 – Visual representation of the results of clustering using the KMeans model with appropriate segments. The data intervals belonging to the window associated with the majority cluster are not colored, while the data intervals associated with the minority cluster are colored in orange. The part of the signal with transitions between two states is colored in wheat (light orange).

The results of the proposed methodology are compared between the features extracted using both the Kaiser window, with its adjustable beta parameter allowing for tailored transition widths, and the commonly used von Hann window (Kara et al., 2005; Tian et al., 2023; Tokmakçi, 2007). The comparative analysis demonstrated that the choice of windowing method did not affect any of the study results or contributions. Specifically, there were no differences in the number of significant features identified, the recovery time following the VR exposure, or the clustering outcomes of the data intervals using ML, regardless of which windowing method was employed.

Discussion

The channel comparison analysis is important for subsequent steps in methodology as statistically significant differences between the channels suggest that each can offer unique and additive information apart from the already used time delay between array recordings of the EGG signal (O'Grady et al., 2010, 2018; Miljković et al., 2023). Conversely, if no significant differences are found, it may be possible to conduct the recording process by reducing the number of channels used, thereby minimizing the complexity of the setup through fewer wires and electrodes. Certainly, this approach relies on dedicated protocols and signal processing. For instance: to compare dominant frequencies in post-prandial and fasting states one channel carries information of interest (Popović et al., 2019a;

Popović, 2021). However, to the best of our knowledge, this is the first time to explore channel information content in terms of CS detection from EGG signals. From the analysis of the results provided in Table 1, it can be seen that even though the Friedman test shows a difference between channels the post-hoc shows no significant difference during pairwise comparison. It can also be remarked that the lowest adjusted *p*-value (0.23) is calculated by comparing ch1 and ch2, while for the other two comparisons, the *p*-value shows a maximum value (1.00). Recording multiple channels does not always provide new information, but investigating the linear relationship between channels seems more interesting. The strongest linear correlation observed between ch1 and ch2 (0.63) points out to some level of linear relationship, whereas the correlations between ch2 and ch3, and ch1 and ch3, suggest minimum to no linear relationship. Contrary to these numerical findings, the visual analysis presented in Figure 3 does not highlight such pronounced differences between channel pairs as suggested by the Pearson coefficients. Also, it can be noticed that all three coefficients are positive which is explained by the direction of the recording vectors described by (Popović, 2021; Miljković et al., 2019). Our analysis, which primarily utilized ch1 for assessing CS, aligns with the support found in the relevant literature (Miljković et al., 2019). However, our examination of statistical tests reveals no significant difference between the channels, suggesting they may derive from the same distribution and thus not necessitate additional processing. Despite this, ch1 has shown promising results (Miljković et al., 2019), affirming its retention for further analysis. Meanwhile, ch2, because of its moderate correlation with ch1 (0.63), does not emerge as a strong candidate due to its similarity. On the contrary, ch3, displaying a low correlation with ch1 (0.13), indicates a divergence that could be beneficial. Thus, the feature selection is also performed on the features combined from both ch1 and ch3 and presented in Table 3 and it could be observed that the combined use of these channels not only supports but also strengthens the outcomes achieved using ch1 alone. Since the results of the test for independent measurements (Mann-Whitney) are shown in Table 3, the analysis is repeated using the test for repeated measurements (Wilcoxon signed-rank). As no difference in the selected features is found when combining features derived from ch1 and ch3, further analysis is conducted using only ch1, as suggested by Miljković et al. (2019). Although there is no unanimous recommendation for the selection of EGG channels,

guided visual observation and manual corrections remain the gold standard for evaluating EGG recordings (Jakus et al., 2022; Gruden et al., 2021; Popović et al., 2019b). While multiple channels can enhance reliability and provide additional information, selecting a single channel offers simplicity in both hardware and processing pipelines. Therefore, ch1 is selected for further analysis to align with previous research (Miljković et al., 2019). A more in-depth analysis of channel selection for CS detection, similar to that proposed by Popović et al. (2019), should be considered in future studies.

During the identification of the features effective for CS detection, our analysis exclusively compares data from B1 and VR1. This comparison strategy ensures that the B1 features are free from any influence of previous VR sessions, confirming that the stomach smooth muscles are in a completely recovered state. It also guarantees that the responses observed during the initial VR exposure are solely due to that particular VR experience, without interference from past exposures. The use of an amplitude seems a good choice as based on the literature the amplitude variations could be used as a short-term indicator of CS (Gruden et al., 2021) and the use of RMS on all decomposition levels proves to be a suitable CS marker. Likewise, in the frequency domain, the normal electrical rhythm of stomach smooth muscles, typically ranging between 2 cpm and 4 cpm, provides a baseline against which deviations can be measured. Disruptions in this rhythm manifest as either slow gastric waves - bradygastria (1-2 cpm) or rapid gastric waves - tachygastria (4-10 cpm), with each offering distinct markers for CS. The published literature confirms that extracting PSD on frequency bands that correspond to bradygastria and tachygastria and monitoring their changes in time could be used to detect changes in EGG that originated from the onset of CS (Miljković et al., 2019; Tian et al., 2023; Dennison et al., 2016). However, statistical analysis reveals that all features extracted from PSD, except the dominant scale, across all wavelet coefficients, serve as a reliable indicator for CS in our study. This finding diverges from the existing literature (Gruden et al., 2021; Miljković et al., 2019; Tian et al., 2023; Popović et al., 2019b), where the dominant frequency is strongly correlated with CS. Since the dominant scale is inspired by this well-established metric, it is expected to be a strong indicator of CS onset, showing that further research is necessary. Conversely, all other examined features demonstrate significant statistical differences (p-value < 0.010) between the B1 and VR1 samples. This uniform significance

across all wavelet coefficients for the remaining features suggests that exploring more decomposition levels could be a promising direction for future research. Consequently, the features related to the dominant scale are excluded from subsequent analyses, with the focus shifting to those features that show statistical significance.

As explained in both methodology and the discussion regarding feature selection, the changes in the protocol which included multiple VR experiences on the same day raise a question of whether the smooth muscles of the stomach had enough time to recover from CS and not corrupt further experiment. The results indicate that 5 data intervals of B2 meet the conditions and can be considered to be the part of B1 distribution. The majority of the B2 segment is considered to be still corrupted by the disturbances and it can be only assumed that the stomach recovery was completed approximation 8 minutes after VR1 cessation. This also indicates a good assumption when conducting feature selection only on B1 and VR1 and that selection involving remaining segments could compromise findings. Although these findings suggest that there is a necessity for longer pauses than 10 minutes to assess if recovery is indeed completed after 8 minutes or if it is mandatory to have longer pauses as proposed by Miljković et al. (2019) and Tian et al. (2023) further research on a larger group of subjects with the same protocol is required, including multiple VR experiences in the same day, but longer pauses within to confirm our claims.

The final step in our methodology is the development of an ML model to discern between two predefined clusters (baseline and VR), due to the absence of labels. Considering that accurately labeling CS symptoms in real-time is challenging due to the lack of reliable methods for real-time detection, unsupervised learning is advocated as a step toward objective estimation of CS symptoms. Assessments typically rely on pre- and post-experience questionnaires like the SSQ, which do not provide the temporal resolution necessary for precise labeling during EGG recording (Tian & Boulic, 2024; Merchant & Kirollos, 2022). While self-reporting scales such as the Fast Motion Sickness Scale (FMS) have been proposed (Dennison et al., 2016, 2019; Merchant & Kirollos, 2022; Tian & Boulic, 2024), these methods are subjective and can introduce bias, as frequent interruptions may disrupt participants' concentration and potentially influence the onset of CS. Considering these limitations, the potential of unsupervised ML emerges as a significant advantage. Unsupervised approaches can

detect intrinsic patterns and variations in EGG signals without relying on potentially unreliable or biased labels, offering a more objective and accurate analysis of CS-related changes in gastric activity. The KMeans model is used to group data intervals in two clusters. From Figure 5 it can be seen that the VR1 segment is considered to be baseline or transient where only one data interval at the beginning of VR1 is grouped as actual VR. In the case of VR2, it can be observed that data intervals belong to VR with transient and CS intervals. The weak link observed between the clusters and VR segments can be attributed to initial assumptions regarding the relationship between CS and VR exposure that require reevaluation. Firstly, it is assumed that the data intervals extracted from the EGG signals would naturally cluster into two distinct groups: baseline and CS. However, our findings suggest that CS manifests in a more nuanced and gradual manner, lacking clear-cut boundaries the states. Future research should explore the possibility of using more than two clusters with the idea of extracting multiple levels of CS or the utilization of different unsupervised models (such as Density-Based Spatial Clustering of Applications with Noise - DBSCAN) which does not predefine the number of clusters (Géron, 2022). Secondly, it is assumed that CS symptoms would be confined to the duration of VR exposure. Contrary to this assumption, studies have shown that CS symptoms can take several minutes to develop after the onset of VR exposure (e.g., approximately 3 minutes during video-watching tasks) and can persist long after the VR experience has ended, sometimes lasting up to several days depending on the individual's susceptibility (Isu et al., 2014; Tian et al., 2023). In our study, it is observed that the feature set distribution from B2 began to resemble B1 only eight minutes after the VR1 session concluded. This delay underscores the extended impact of CS beyond the VR session itself, suggesting that CS is not strictly bounded by VR experience. Nevertheless, this step shows promising and interesting results regarding stomach recovery and automatic CS detection in EGG signals.

In examining the MLs role in CS detection, the literature review highlights two approaches: the utilization of EEG features as a sole indicator, and the multimodal approach consisting of a combination of features extracted from physiological and behavioral signals including ECG, EGG, posture, EDA, etc. (Yang et al., 2022; Keshavarz et al., 2022). A common objective in these studies is the prediction of CS severity, typically determined through the SSQ (before and/or after the simulation) or ver-

bal estimations of symptoms during the simulation. While EGG features have not been widely recognized as standalone indicators for CS or nausea, recent studies integrating EGG in multimodal ML models have yielded substantial accuracy. Keshavarz et al. (2022) developed a multimodal ML model for real-time estimation of visually induced MS (which is a synonym for CS) and the classification of subjects whether they experience sickness or not during the simulation. This approach uses EGG features as an indicator but concludes that EGG features alone showed only a weak link with the majority of CS measurements. Similarly, Dennison et al. (2019) shows that a model based only on EGG achieved an accuracy of 48% for multiclass classification of symptoms during the simulation, but in combination with different features achieved an accuracy of 95%. In our opinion, nausea as one of the most specific symptoms of CS is inherently linked to the smooth muscles of the stomach, which EGG directly captures. This connection underpins our hypothesis that EGG data harbors valuable insights into nausea and CS manifestations. Supporting this notion is the study conducted by Jakus et al. (2022), which reports an 88% accuracy rate in nausea detection, proving the premise that with innovative and creative feature engineering, EGG can indeed serve as a reliable source of information for CS assessment. All available ML-based research reports used label information about CS and trained their model in a supervised manner with reliable evaluation metrics. Conversely, an unsupervised ML approach is employed for segmentation and the direct comparison with the established literature could not be performed due to the lack of evaluation metrics. Future research should not only expand the participant pool but also enable a robust comparative analysis with our work and validate the findings.

Contribution of the study

Our study, which focuses on a single participant and employed an innovative protocol using EGG recordings to explore CS during VR sessions, yields insights into the initial research questions:

1. It is found that traditional and wavelet-based features effectively indicate CS segments within the signal. However, features related to the dominant scale do not demonstrate significant differences, neither in the signal nor in the wavelet coefficients.

2. Statistical tests reveal no significant differences across channels. Additionally, the Pearson correlation coefficients indicate a medium linear correlation between ch1 and ch2, while the remaining two coefficients achieve low to no linear correlation.
3. The unsupervised ML model shows promising results in detecting the segments of the signal affected by the CS.

An additional contribution of our study is the finding that the choice between the Kaiser and von Hann window functions did not significantly impact the identification of significant features, the recovery patterns following VR1, or the segmentation outcomes in CS detection using machine learning methods.

Limitations of the study

We recognize the following limitations and propose directions for future research:

1. Although this study offers valuable preliminary findings, it is based on a single case study which may limit the generalizability of our findings due to potential individual differences in anatomical, physiological, or psychological characteristics. Future research with a larger study group is necessary to confirm these findings, enabling robust statistical analyses that can clarify trends and minimize the possibility of misleading results caused by individual variability.
2. Wavelet-based features are proved to be important parameters in the detection of CS and further exploration of different wavelets apart from Daubechies and different levels of decomposition may be considered for future research.
3. This paper only investigates linear correlations between different channels of EGG, but appropriate analysis to reveal potential nonlinear relations could be explored in the future.
4. The extension of the feature set (*e.g.*, entropy, crest factor as well as max, mean, and min values of each DWT coefficient) Miljković et al. (2019); Jakus et al. (2022); Tokmakçi (2007) could be investigated for CS detection.
5. The weak link between the clusters and VR segments (25% for VR1 and 50% for VR2) suggests that data intervals could not be naturally clustered into two distinct groups (baseline and CS), as well as

that CS symptoms would be confined to the duration of VR exposure, highlighting the need for improved evaluation of clustering and determination of cluster number in future research.

6. The more compelling comparative analysis of unsupervised models, including ones without the predefined number of clusters such as DBSCAN, could be included in future work as well as different appropriate metrics for clusterization analysis.
7. The duration of the segments used in this study is relatively short. It should be noted that for EGG measurements it is typically recommended to measure 15 minutes or more (Stern et al., 1987; Parkman et al., 2003). On the other hand, our approach enables quasi-real-time analysis, which is not feasible with protocols that involve relatively long signal measurements. In support of our approach, the detection of sickness onset can be performed almost immediately with the application of amplitude threshold in the time domain (Gruden et al., 2021).
8. This research only explored two window functions (Kaiser and von Hann), and future studies should expand the investigation by examining how different window function selections influence the feature extraction process in EGG signal analysis.

Conclusion

Our investigation into CS through EGG recordings during VR sessions, despite being conducted with a single participant and employing a non-traditional protocol, has yielded significant insights. The statistical analyses reveal no significant differences between channels, suggesting uniformity in the EGG signal response to CS across different recordings. Meanwhile, the correlation analysis reveals a moderate linear correlation (0.63) between ch1 and ch2, whereas the other two pairs exhibit low to negligible linear correlation. It is found that the RMS of the EGG amplitude, the maximum value of PSD, and the mean value of PSD across all DWT coefficients could be used for the detection of CS resulting in 15 significant features. The observations of stomach recovery are evident 8 minutes after the VR experience confirming no necessity for longer pauses between VR experiences. Lastly, the application of an unsupervised ML model demonstrates potential in identifying CS-affected signal segments, indicating a fruitful di-

rection for future research involving a broader exploration of unsupervised ML techniques in this context.

Statement

During the preparation of this work, the author(s) used GPT4 (ChatGPT) in order to improve readability and language. After using this tool/service, the author(s) reviewed and edited the content as needed and take(s) full responsibility for the content of the publication.

References

Akansu, A.N. & Haddad, R.A. 2001. *Multiresolution signal decomposition: Transforms, subbands, and wavelets, 2nd Edition*. San Diego: Academic Press. ISBN 978-0-12-047141-6.

Bruzzone, A.G. & Massei, M. 2017. Simulation-Based Military Training. In: *Mittal, S., Durak, U. & Ören, T. (Eds.) Guide to Simulation-Based Disciplines. Simulation Foundations, Methods and Applications.* pp. 315–361. Cham: Springer. Available at: https://doi.org/10.1007/978-3-319-61264-5_14.

Cacioppo, J.T., Tassinary, L.G. & Berntson, G. 2007. *Handbook of psychophysiology*. Cambridge University Press. ISBN 9781139461931.

Dennison, M.S., D'Zmura, M., Harrison, A.V., Lee, M. & Raglin, A.J. 2019. Improving motion sickness severity classification through multi-modal data fusion. In: *Pham, T. (Eds.) Proceedings Artificial Intelligence and Machine Learning for Multi-Domain Operations Applications*. Vol. 11006, art.number:110060T. Available at: https://doi.org/10.1117/12.2519085.

Dennison, M.S., Zachary Wisti, A. & D'Zmura, M. 2016. Use of physiological signals to predict cybersickness. *Displays*, 44, pp. 42–52. Available at: https://doi.org/10.1016/j.displa.2016.07.002.

Gruden, T., Popović, N.B., Stojmenova, K., Jakus, G., Miljković, N., Tomažič, S. & Sodnik, J. 2021. Electrogastrography in Autonomous Vehicles—An Objective Method for Assessment of Motion Sickness in Simulated Driving Environments. *Sensors*, 21(2), art.number:550. Available at: https://doi.org/10.3390/s21020550.

Géron, A. 2022. *Hands-On Machine Learning with Scikit-Learn, Keras, and TensorFlow (3rd ed)*. Sebastopol, California: O'Reilly Media, Inc. ISBN 9781098122478.

Harris, C.R., Millman, K.J., Van Der Walt, S.J., Gommers, R., Virtanen, P., Cournapeau, D., Wieser, E., Taylor, J., Berg, S., Smith, N.J., Kern, R., Picus, M., Hoyer, S., Van Kerkwijk, M.H., Brett, M., Haldane, A., Del Río, J.F., Wiebe, M., Peterson, P., Gérard-Marchant, P., Sheppard, K., Reddy, T., Weckesser, W.,

Abbasi, H., Gohlke, C. & Oliphant, T.E. 2020. Array programming with NumPy. *Nature*, 585, pp. 357–362. Available at: https://doi.org/10.1038/s41586-020-2649-2.

Hunter, J.D. 2007. Matplotlib: A 2D Graphics Environment. *Computing in Science & Engineering*, 9(3), pp. 90–95. Available at: https://doi.org/10.1109/MCSE.2007.55.

Isu, N., Hasegawa, T., Takeuchi, I. & Morimoto, A. 2014. Quantitative analysis of time-course development of motion sickness caused by in-vehicle video watching. *Displays*, 35(2), pp. 90–97. Available at: https://doi.org/10.1016/j.displa.2014.01.003.

Jakus, G., Sodnik, J. & Miljković, N. 2022. Electrogastrogram-Derived Features for Automated Sickness Detection in Driving Simulator. *Sensors*, 22(22), art.number:8616. Available at: https://doi.org/10.3390/s22228616.

Kaiser, J. & Schafer, R. 1980. On the use of the I0-sinh window for spectrum analysis. *IEEE Transactions on Acoustics, Speech, and Signal Processing*, 28(1), pp. 105–107. Available at: https://doi.org/10.1109/TASSP.1980.1163349.

Kara, S., Dirgenali, F. & Okkesim, S. 2005. Estimating Gastric Rhythm Differences Using a Wavelet Method from the Electrogastrograms of Normal and Diabetic Subjects. *Instrumentation Science & Technology*, 33(5), pp. 519–532. Available at: https://doi.org/10.1080/10739140500222907.

Keshavarz, B. & Hecht, H. 2011. Validating an Efficient Method to Quantify Motion Sickness. *Human Factors: The Journal of the Human Factors and Ergonomics Society*, 53(4), pp. 415–426. Available at: https://doi.org/10.1177/0018720811403736.

Keshavarz, B., Peck, K., Rezaei, S. & Taati, B. 2022. Detecting and predicting visually induced motion sickness with physiological measures in combination with machine learning techniques. *International Journal of Psychophysiology*, 176, pp. 14–26. Available at: https://doi.org/10.1016/j.ijpsycho.2022.03.006.

Kim, Y.Y., Kim, H.J., Kim, E.N., Ko, H.D. & Kim, H.T. 2005. Characteristic changes in the physiological components of cybersickness. *Psychophysiology*, 42(5), pp. 616–625. Available at: https://doi.org/10.1111/j.1469-8986.2005.00349.x.

Kuhl, J., Evans, D., Papelis, Y., Romano, R. & Watson, G. 1995. The Iowa Driving Simulator: an immersive research environment. *Computer*, 28(7), pp. 35–41. Available at: https://doi.org/10.1109/2.391039.

LaViola, J.J. 2000. A discussion of cybersickness in virtual environments. *ACM SIGCHI Bulletin*, 32(1), pp. 47–56. Available at: https://doi.org/10.1145/333329.333344.

Lee, B.H. & Kuo, S. 2001. *Real-Time Digital Signal Processing: Implementaions, Applications and Experiements with the TMS320C55X.* Wiley Hoboken, NJ, USA. ISBN 1-280-55452-5.

McKinney, W. 2010. Data Structures for Statistical Computing in Python. In: *Van der Walt, S. & Millman, J. (Eds.) Proceedings of the 9th Python in Science Conference*. Austin, Texas, pp.56-61, June 28 - July 3. Available at: https://doi.org/10.25080/Majora-92bf1922-00a.

McKnight, P.E. & Najab, J. 2010. Mann-Whitney U Test. *The Corsini Encyclopedia of Psychology*. 30 January. Available at: https://doi.org/10.1002/9780470479216.corpsy0524.

Merchant, W. & Kirollos, R. 2022. An Overview of Cybersickness Self-Report Measures for use in Defence Research and Development Canada Experiments, Reference Document DRDC-RDDC-2022-D063. *Defence Research and Development Canada*. [online]. Available at: https://cradpdf.drdc-rddc.gc.ca/PDFS/unc392/p814963_A1b.pdf [Accessed: 10 June 2024].

Meta. 2024. *Epic Roller Coasters* [online]. Available at: https://www.meta.com/experiences/pcvr/epic-roller-coasters/1477883658957255/#reviews [Accessed: 10 June 2024].

Miljković, N., Popović, N.B., Prodanov, M. & Sodnik, J. 2019. Assessment of sickness in virtual environments. In: *Konjović, Z., Zdravković, M. & Trajanović, M. (Eds.) Proceedings of the 9th International Conference on Information Society and Technology (ICIST 2019)*. Kopaonik, Serbia, pp.76-81, March 10-13 [online]. Available at: https://www.eventiotic.com/eventiotic/files/Papers/URL/f412a358-82d8-46aa-b0c9-6ad30de5890d.pdf [Accessed: 10 June 2024] ISBN: 978-86-85525-24-7.

Miljković, N., Popović, N.B. & Sodnik, J. 2023. Electrogastrogram Signal Processing: Techniques and Challenges with Application for Simulator Sickness Assessment. In: *Biomedical Signal Processing, 1st Edition*, pp.62-89. CRC Press [online]. Available at: https://www.taylorfrancis.com/chapters/edit/10.1201/9781003201137-4/electrogastrogram-signal-processing-nadica-miljkovi%C4%87-nenad-popovi%C4%87-jaka-sodnik [Accessed: 10 June 2024] ISBN: 9781003201137.

Miljković, N. & Sodnik, J. 2023. Towards Objective Assessment of Driving Simulation Sickness: Pros and Cons of Stomach Electrical Activity. In: *Kemeny, A., Chardonnet, J.-R. & Colombet, F. (Eds.) Proceedings of the Driving Simulation Conference 2023 Europe VR*. Antibes Juan-les-Pins, France, pp.81-88, September 6-8 [online]. Available at: https://proceedings.driving-simulation.org/proceeding/dsc-2023/towards-objective-assessment-of-driving-simulation-sickness-pros-and-cons-of-stomach-electrical-activity/ [Accessed: 10 June 2024] ISBN: 978-2-9573777-3-2.

NATO Science and Technology Office. 2021. *Guidelines for Mitigating Cybersickness in Virtual Reality Systems. Peer-reviewed Final Report of the Human Factors and Medicine Panel/Modeling and Simulations Group, Activity Number 323 (NATO STO-TR-HFM-MSG-323)* [online]. Available at: https://apps.dtic.mil/sti/pdfs/AD1183673.pdf [Accessed: 10 June 2024].

O'Grady, G., Angeli, T.R., Paskaranandavadivel, N., Erickson, J.C., Wells, C.I., Gharibans, A.A., Cheng, L.K. & Du, P. 2018. Methods for High-Resolution Electrical Mapping in the Gastrointestinal Tract. *IEEE Reviews in Biomedical Engineering*, 12, pp. 287–302. Available at: https://doi.org/10.1109/RBME.2018.2867555.

O'Grady, G., Du, P., Cheng, L.K., Egbuji, J.U., Lammers, W.J.E.P., Windsor, J.A. & Pullan, A.J. 2010. Origin and propagation of human gastric slow-wave activity defined by high-resolution mapping. *American Journal of Physiology-Gastrointestinal and Liver Physiology*, 299(3), pp. G585–G592. Available at: https://doi.org/10.1152/ajpgi.00125.2010.

Oppenheim, A.V. 2008. *Discrete-time Signal Processing, 2nd Edition*. Pearson Education. ISBN 9788131704929.

Parkman, H.P., Hasler, W.L., Barnett, J. & Eaker, E. 2003. Electrogastrography: a document prepared by the gastric section of the American Motility Society Clinical GI Motility Testing Task Force. *Neurogastroenterology & Motility*, 15(2), pp. 89–102. Available at: https://doi.org/10.1046/j.1365-2982.2003.00396.x.

Pedregosa, F., Varoquaux, G., Gramfort, A., Michel, V., Thirion, B., Grisel, O., Blondel, M., Prettenhofer, P., Weiss, R., Dubourg, V., Vanderplas, J., Passos, A., Cournapeau, D., Brucher, M., Perrot, M. & Duchesnay, E. 2011. Scikit-learn: Machine Learning in Python. *Journal of Machine Learning Research*, 12, pp. 2825–2830 [online]. Available at: https://www.jmlr.org/papers/volume12/pedregosa11a/pedregosa11a.pdf [Accessed: 10 June 2024].

Percival, D.B. & Walden, A.T. 2006. *Wavelet Methods for Time Series Analysis (Cambridge Series in Statistical and Probabilistic Mathematics, Series Number 4)*. Cambridge University Press. ISBN 9780521685085.

Popović, N.B. 2021. *Methods for assessment of electrical activity of smooth muscles*. Phd thesis, Belgrade, Serbia: University of Belgrade, School of Electrical Engineering. [online]. Available at: https://nardus.mpn.gov.rs/handle/123456789/18615 [Accessed: 10 June 2024].

Popović, N.B., Miljković, N. & Popović, M.B. 2019a. Simple gastric motility assessment method with a single-channel electrogastrogram. *Biomedical Engineering/Biomedizinische Technik*, 64(2), pp. 177–185. Available at: https://doi.org/10.1515/bmt-2017-0218.

Popović, N.B., Miljković, N., Stojmenova, K., Jakus, G., Prodanov, M. & Sodnik, J. 2019b. Lessons Learned: Gastric Motility Assessment During Driving Simulation. *Sensors*, 19(14), art.number:3175. Available at: https://doi.org/10.3390/s19143175.

Seabold, S. & Perktold, J. 2010. Statsmodels: Econometric and Statistical Modeling with Python. In: *Van der Walt, S. & Millman, J. (Eds.) Proceedings of the 9th Python in Science Conference*. Austin, Texas, pp.92-96, June 28-July 3. Available at: https://doi.org/10.25080/Majora-92bf1922-011.

Stern, R.M., Koch, K.L., Stewart, W.R. & Lindblad, I.M. 1987. Spectral analysis of tachygastria recorded during motion sickness. *Gastroenterology*, 92(1), pp. 92–97. Available at: https://doi.org/10.1016/0016-5085(87)90843-2.

Tecknotrove. 2023. Role of defense simulator training in enhancing national security. *Tecknotrove.com*, 26 September [online]. Available at: https://tecknotrove.com/role-of-defence-simulator-training-in-national-security/ [Accessed: 10 June 2024].

Tian, N., Achache, K.H., Ben Mustapha, A.R. & Boulic, R. 2023. EGG Objective characterization of cybersickness symptoms towards navigation axis. In: *2023 IEEE Conference on Virtual Reality and 3D User Interfaces Abstracts and Workshops (VRW)*. Shanghai, China, pp.289-297, March 25-28. Available at: https://doi.org/10.1109/VRW58643.2023.00068.

Tian, N. & Boulic, R. 2024. Who says you are so sick? An investigation on individual susceptibility to cybersickness triggers using EEG, EGG and ECG. *IEEE Transactions on Visualization and Computer Graphics*, 30(5), pp. 2379–2389. Available at: https://doi.org/10.1109/TVCG.2024.3372066.

Tokmakçi, M. 2007. Analysis of the Electrogastrogram Using Discrete Wavelet Transform and Statistical Methods to Detect Gastric Dysrhythmia. *Journal of Medical Systems*, 31(4), pp. 295–302. Available at: https://doi.org/10.1007/s10916-007-9069-9.

Valens, C. 1999. *A really friendly guide to wavelets*. [online]. Available at: https://www.cs.unm.edu/~williams/cs530/arfgtw.pdf [Accessed: 10 June 2024].

Van Rossum, G. & Drake, F.L. 1995. *Python reference manual, Release 2.1.1.* Amsterdam, The Netherlands: Stichting Mathematisch Centrum. ISBN 1441412697.

Virtanen, P., Gommers, R., Oliphant, T.E., Haberland, M., Reddy, T., Cournapeau, D., Burovski, E., Peterson, P., Weckesser, W., Bright, J., van der Walt, S.J., Brett, M., Wilson, J., Millman, K.J., Mayorov, N., Nelson, A.R.J., Jones, E., Kern, R., Larson, E., Carey, C.J., Polat, I., Feng, Y., Moore, E.W., VanderPlas, J. & SciPy1.0Contributors. 2020. SciPy 1.0: fundamental algorithms for scientific computing in Python. *Nature methods*, 17, pp. 261–272. Available at: https://doi.org/10.1038/s41592-019-0686-2.

Vlačić, S.I., Knežević, A.Z., Mandal, S., Rođenkov, S. & Vitsas, P. 2020. Improving the pilot selection process by using eye-tracking tools. *Journal of Eye Movement Research*, 12(3). Available at: https://doi.org/10.16910/jemr.12.3.4.

Woolson, R.F. 2005. Wilcoxon Signed-Rank Test. In: *Encyclopedia of Biostatistics*. 15 July. Available at: https://doi.org/10.1002/0470011815.b2a15177.

Yang, A.H.X., Kasabov, N. & Cakmak, Y.O. 2022. Machine learning methods for the study of cybersickness: a systematic review. *Brain Informatics*, 9, art.number:24. Available at: https://doi.org/10.1186/s40708-022-00172-6.

Electrogastrograma-detección de la ciberenfermedad mediante la aplicación de la transformación wavelet y el aprendizaje automático: estudio de caso

Ilija V. Tanasković[a,b], **autor de correspondencia**, *Nenad* B. Popović[a], *Jaka* J. Sodnik[c], *Sašo* J. Tomažič[c], *Nadica* S. Miljković[a,c]

[a] Universidad de Belgrado, Facultad de Ingeniería Eléctrica, Belgrado, República de Serbia

[b] Instituto de Investigación y Desarrollo de Inteligencia Artificial de Serbia, Novi Sad, República de Serbia

[c] Universidad de Liubliana, Facultad de Ingeniería Eléctrica, Liubliana, República de Eslovenia

CAMPO: electrónica, tecnologías de información

TIPO DE ARTÍCULO: artículo científico original

Resumen:

Introducción/objetivo: La aplicación de tecnologías de realidad virtual (RV) y simulación en el entrenamiento militar ofrece un enfoque rentable y versátil para mejorar el entrenamiento. Sin embargo, la prevalencia de la ciberenfermedad (CS), caracterizada por síntomas como náuseas, limita su uso generalizado.

Métodos: Este estudio introduce parámetros objetivos para la detección de CS utilizando el registro de electrogastrograma (EGG) de tres canales de un sujeto específico y evalúa la independencia y correlación lineal para la selección apropiada del canal. El artículo emplea una transformación wavelet discreta de 3 niveles (DWT) en el canal elegido para identificar parámetros clave indicativos de trastornos gástricos. Además, el artículo investiga la recuperación de CS después de VR y examina la aplicación de aprendizaje automático (ML) no supervisado para segmentar EGG en línea base y CS, utilizando características significativas identificadas previamente.

Resultados: El análisis no revela diferencias significativas entre los canales EGG y una correlación lineal moderada a baja entre pares de canales. La selección de características demuestra que la raíz cuadrada media de la amplitud, así como los valores máximos y medios de la densidad espectral de potencia (PSD) calculados en todos los coeficientes DWT son efectivos para la detección de CS, mientras que la escala EGG dominante no pudo indicar CS para ningún nivel de descomposición. Además, los signos de recuperación aparecen aproximadamente 8 minutos después de la primera experiencia de VR, lo que respalda

la idea de realizar múltiples sesiones el mismo día, es decir, un entrenamiento intensivo basado en VR.

Conclusión: El ML no supervisado muestra potencial en la identificación de segmentos de señales EGG afectados por CS con extracción de características basada en DWT, ofreciendo un enfoque novedoso para mejorar la prevención de la aparición de CS en el entrenamiento militar basado en VR y otros entornos relacionados con VR.

Palabras claves: ciberenfermedad, transformada wavelet discreta, electrogastrografía (EGG), selección de características, aprendizaje automático, entrenamiento militar, densidad espectral de potencia, realidad virtual.

Обнаружение симптомов киберболезни на основании электрогастрограммы с применением вейвлет-преобразования и машинного обучения: целевое исследование

Илья В. Танаскович[а,б], **корреспондент**, *Ненад* Б. Попович[а], *Яка* Й. Содник[в], *Сашо* Й. Томажич[в], *Надица* С. Милькович[а,в]

[а] Белградский университет, электротехнический факультет, г. Белград, Республика Сербия

[б] Институт исследований и разработок в области искусственного интеллекта Сербии, г. Нови-Сад, Республика Сербия

[в] Люблянский университет, факультет электротехники, г. Любляна, Республика Словения

РУБРИКА ГРНТИ: 28.17.33 Компьютерное моделирование реальности. Виртуальная реальность

ВИД СТАТЬИ: оригинальная научная статья

Резюме:

Введение/цель: Применение виртуальной реальности (ВР) и симуляторов обеспечивает экономичный и интуитивно понятный подход к боевой подготовке. Однако из-за тошноты, возникающей в процессе учений на симуляторе (симптомы тошноты – СТ), ограничивает их в более широком применении.

Методы: В данном исследовании представлены объективные параметры обнаружения СТ с использованием трехканальной электрогастрограммы (ЭГГ), записанной у одного

респондента, а также оценена независимость и линейная корреляция для соответствующего выбора одного канала. В статье к выбранному каналу ЭГГ применялось дискретное вейвлет-преобразование (ДВП) с тремя уровнями с целью выявления ключевых особенностей, указывающих на дисфункцию желудка. Помимо того, в ходе исследования оценивалось восстановление после СМ, вызванных использованием ВР, и анализировалось применение неконтролируемого машинного обучения (МО) для сегментации ЭГГ на базовый сегмент и сегмент во время СТ, используя важные особенности, выявленные ранее.

Результаты: Проведенный анализ не выявил существенных различий между тремя каналами ЭГГ. Однако была выявлена линейная корреляция (от умеренной к низкой) между парами каналов. Выбор признаков демонстрирует, что среднеквадратичное значение амплитуды, а также максимальное и среднее значения спектральной плотности мощности (СПМ), рассчитанные по всем коэффициентам ДВП, эффективны для обнаружения СТ, в то время как доминирующая шкала ЭГГ не может указывать СТ ни на одном уровне декомпозиции. Помимо того, признаки восстановления проявляются примерно через 8 минут после первого использования виртуальной реальности, что подтверждает идею о проведении нескольких сеансов обучения в один и тот же день, т.е. интенсивные учения в среде виртуальной реальности возможны.

Выводы: Применение неконтролируемого МО может идентифицировать сегменты ЭГГ во время СТ с извлечением функций на основании ДВП, предлагая новый подход к предотвращению СТ в боевой подготовке в среде виртуальной реальности, а также в других средах, связанных с технологией ВР.

Ключевые слова: киберболезнь, дискретное вейвлет-преобразование, электрогастрография (ЭГГ), выбор признаков, машинное обучение, военная подготовка, спектральная плотность мощности, виртуальная реальность.

Детекција симптома изазваних коришћењем симулатора заснована на електрогастрографском сигналу уз примену дискретне трансформације таласићима и машинског учења: студија случаја

Илија В. Танасковић[а,б], **аутор за преписку**, *Ненад* Б. Поповић[а], *Јака* Ј. Содник[в], *Сашо* Ј. Томажич[в], *Надица* С. Миљковић[а,в]

[а] Универзитет у Београду, Електротехнички факултет, Београд, Република Србија

[б] Истраживачко-развојни институт за вештачку интелигенцију, Нови Сад, Република Србија

[в] Универзитет у Љубљани, Електротехнички факултет, Љубљана, Република Словенија

ОБЛАСТ: електроника, информационе технологије
КАТЕГОРИЈА (ТИП) ЧЛАНКА: оригинални научни рад

Сажетак:

Увод/циљ: Примена виртуелне реалности (ВР) и симулатора пружа исплатив и интуитиван приступ војној обуци. Међутим, могућност појаве мучнине, која је изазвана коришћењем симулатора (симптома мучнине – СМ), ограничава њихову ширу примену.

Методе: Ово истраживање уводи објективне параметре за детекцију СМ, коришћењем троканалног електрогастрограма (ЕГГ) снимљеног на једном испитанику, и процењује независност и линеарну корелацију за одговарајући избор једног канала. Примењена је дискретна трансформација таласићима (ДТТ) са три нивоа на изабрани ЕГГ канал, како би се идентификовала кључна обележја која указују на поремећај рада желуца. Поред тога, евалуиран је опоравак након СМ, настао услед коришћења ВР, а анализирана је и примена машинског учења (МУ) без надгледања за сегментацију ЕГГ на основни сегмент и сегмент током СМ, коришћењем претходно идентификованих обележја од значаја.

Резултати и дискусија: Анализа показује да нема значајних разлика између три ЕГГ канала, као и умерену до ниску линеарну корелацију између парова канала. Избор обележја сугерише да се применом средње квадратне вредности амплитуде, као и максималне и просечне вредности спектралне густине снаге (СГС), израчунате на свим ДТТ коефицијентима, успешно детектује СМ, док примена доми-

Tanasković, I. et al., Electrogastrogram-based detection of cybersickness with the application of wavelet transformation and..., pp.79–114

нантне скале ЕГГ није указала на присуство СМ ни за један ниво декомпозиције. Поред тога, показано је да се знаци опоравка појављују приближно 8 минута након првог ВР искуства, што указује на то да се више ВР сесија може спровести истог дана, односно да је интензивна ВР обука могућа.

Закључак: Примена МУ без надгледања има потенцијал у идентификацији ЕГГ сегмената током СМ уз издвајање обележја заснованих на ДТТ, нудећи нови приступ у превенцији појаве СМ у војној обуци заснованој на ВР, као и другим областима повезаним са ВР технологијом.

Кључне речи: симптоми мучнине, дискретна трансформација таласићима, електрогастрографија, одабир обележја, машинско учење, војна обука, спектрална густина снаге, виртуелна реалност.

Paper received on: 11.06.2024.
Manuscript corrections submitted on: 27.01.2025.
Paper accepted for publishing on: 28.01.2025.